

## SIMULATING THE DRYING KINETICS OF CASSAVA FLOUR IN A LABORATORY MODEL DRYER USING FINITE DIFFERENCE METHOD

O. A. Adejumo<sup>1\*</sup> and K. Oje<sup>2</sup>

<sup>1</sup>National Centre for Agricultural Mechanization, Idofian, Ilorin, Kwara State, Nigeria

<sup>2</sup>Department of Agricultural and Bio-systems Engineering, University of Ilorin, Ilorin, Kwara State, Nigeria)

\*Corresponding author's e-mail address: [oluyemisi123@gmail.com](mailto:oluyemisi123@gmail.com)

### Abstract

Mathematical models were developed to describe drying kinetics in the particles of grated unfermented cassava mash during drying to produce high quality cassava flour. Finite difference method was adopted to solve the resulting equations from which a computer programme named “crop simulator 1.0” was developed.

Drying kinetics of grated unfermented cassava mash was investigated experimentally at air temperatures of 40°C, 55°C, 70°C, 85°C and 100°C using a model laboratory dryer. Model validation was carried out using root mean square difference between the experimental values and the simulated values and the result was 0.59% which was within the acceptable limit of 10%. This showed a reasonably close agreement indicating that the crop-drying simulator 1.0 was capable of simulating the drying kinetics.

**Keywords:** Drying kinetics, High quality cassava flour; Finite difference; Crop drying simulator

### 1. Introduction

Cassava is a root crop with excellent source of carbohydrates. It's bulky in nature (containing about 70% moisture), highly perishable, low protein with free amino acid content and high content of the poisonous cyanogenic glucosides (CNG). It is widely recognized as a productive crop and a good energy source with high drought tolerance and low demand for nutrients (Osakwe *et al.*, 2008). After rice and maize, cassava is the third most important food source in the tropics (Cock, 1985). Processing of cassava roots into different end products through drying provides a means of producing shelf stable products for value addition to cassava (Ajala, 2012) and also, preserve cassava root for exportation in a longer storage form which minimizes qualitative and quantitative losses thereby ensures steady production and availability (Adebayo *et al.*, 2009). High quality cassava flour is a cassava product produced from grated unfermented cassava mash. The production process of High Quality Cassava flour from grated unfermented cassava mash involves drying under different parameters without uttering the quality (Adejumo *et al.*, 2011). Evaluating the drying kinetic as a function of drying conditions helps in drying simulation for predicting the suitable drying conditions that will retain quality (Bhagwati, 2011). Simulation results and information on drying kinetics of food products such as drying rates, time-temperature-moisture content distributions, as well as theoretical and empirical approaches to moisture movement, are very essential for the prevention of quality degradation and for the achievement of fast and effective drying. (Mujumdar, 2006).

Drying is widely used in the preservation of cassava and its products but a scientific approach has not so widely been applied (Gatea, 2011). The traditional techniques are often used to set up industrial production, particularly in small and medium scale industries. The formulation of sufficient mathematical drying models to optimize drying process can enhance product quality, reduced process cost, improve speed and decrease the time taken to share information and make critical decision. The mathematical model using partial differential equation (PDE) is a helpful tool that can be used to estimate the drying rate at any moisture condition of a material and to estimate drying time for particular task during drying (Doymaz, 2010). Computer simulation is a powerful tool for measuring changes in temperature and moisture during drying process (Islam, 2010). The increasing development of computer program had a great impact on the quality evaluation of agricultural products (Datta, 2008). Invention of the computer

also influenced the field of numerical analysis, by aiding the solving of longer and more complicated calculations. Therefore, the objectives of this study are: (i) To simulate moisture content versus time in the drying process of high quality industrial cassava flour based on convection-diffusion model using partial difference equation (PDE) and (ii) To provide solution to the derived partial differential equation using finite difference method (iii) to compare the data predicted by the model with the data from the experiment (Shahari, 2012).

Several studies have been conducted on finite difference modeling of drying of cereal (Yahaya, 1979 and Patil, 1988). A number of studies have been reported on finite difference modeling of heating and drying of food materials. However, little or no studies have been reported on finite difference modeling of drying of unfermented cassava mash to produce high quality cassava flour. Two methods are commonly applied to model heat and mass transfer: the finite difference method and the finite element method. The basic ideal of finite difference method is solving partial differential equations by replacing the spatial and time derivatives with suitable approximations (Jeffrey, 2011). In all numerical solutions the continuous partial differential equation (PDE) is replaced with a discrete approximation. In this context the word "discrete" means that the numerical solution is known only at a finite number of points in the physical domain. In general, increasing the number of points not only increases the resolution (i.e., detail), but also the accuracy of the numerical solution. The discrete approximation results into a set of algebraic equations that are solved in order to determine the values of the discrete unknowns.

## **2. Finite difference modelling of grated unfermented cassava mash to produce high quality industrial cassava flour.**

The course and time of drying process depend on the drying conditions, temperature and moisture profile developed by the moisture movement within the material. The major factors affecting the moisture transport during drying can be classified as the external factors and internal factors. (Krzysztof and Agnieszka, 2009).

The external factors are the factors related to the properties of the surrounding air such as temperature, pressure, humidity, velocity and area of the exposed surface, while the internal factors are the parameters related to the properties of the material such as moisture diffusivity, moisture transfer coefficient, water activity, structure and composition (Dincer and Hussain, 2004). In this study, the internal factors were only considered for the modeling of the drying process of cassava mash. Luikov's transport equation described water movement inside the dried solid as only a diffusion movement in the convection drying process of porous product. Luikov's mathematical model was used in modeling of the moisture movement within the particles of the grated unfermented cassava mash and it is expressed as shown in equation (1) (Bhagwati, 2011):

$$\frac{dm}{dt} = \nabla^2 k_{11} M \quad (1)$$

where:  $K_{11}$ =Phenomenological coefficient, M= moisture content (% db).

### **2.1 Formulation of Equation**

Crank Nicolson 1993, analyzed the Luikov's equation and simplified equation (1) into the moisture diffusion equation which is as shown in equation (2) and average moisture content that is revealed in equation (3) based on the following assumptions that:

- i. shape and volume of dried particles do not change, and
- ii. water diffusion coefficient is constant.

$$\frac{\partial M}{\partial t} = D_{eff}(M, \theta) \left[ \frac{n}{r} \frac{dm}{dr} + \frac{d^2m}{dr^2} \right] \quad (2)$$

$$\bar{M} = \frac{3}{R^3} \int_{R=0}^R Mr^2 dr \quad (3)$$

where:  $D_{eff}$  = effective moisture diffusivity ( $m^2/s$ ),  $t$  = time (h),  $n$  = constant and it's dependent of shape of material: 0 for planar geometry, 1 for cylindrical geometry and 2 for spherical geometry,  $r$  = radial position (m),  $\theta$  = grain temperature ( $^{\circ}C$ ) and  $\bar{M}$  = Average moisture content.

Equation (2) is a diffusive equation describing the mass transfer process and has been extensively applied (Jia *et al.*, 2002, Yang *et al.*, 2002, Gason *et al.*, 2002, Rafiee *et al.*, 2007).

### **2.2.1 Model Assumption.**

The following assumptions which were based mostly on literature review aided the model development.

1. The particles of the grated unfermented cassava mash have uniform moisture content and temperature implying uniform moisture distribution and internal heat generation.
2. The particles of the grated unfermented cassava mash are homogenous in nature.
3. The moisture movement within the particles is radial.
4. The mechanism of the drying process is predominantly controlled by liquid diffusion.
5. The temperature within the particles of the grated unfermented cassava mash and shrinkage of the particle are negligible. Therefore, they are not put into consideration in this study.
6. The particles of grated unfermented cassava mash were assumed to be spherical. According to Moorthy (2002), cassava starch granules are mostly round with a flat surface on one side containing a conical pit, which extends to a well-defined eccentric hilum under microscopic examination. Generally, granule size of cassava starch is express as spherical (Adejumo, 2011).

### **2.1.2 Formulation of Equation**

An accurate description of bulk drying rates depends largely on an accurate description of the moisture movement within the individual particles of the agricultural materials (Patil, 2006). Sphere of equivalent radius were assumed to lose moisture by diffusion (Crank, 1998). Based on this and the assumptions, the diffusion of moisture within the particle of the grated unfermented cassava mash and the average moisture content at a unit time interval were analyzed in spherical coordinate using Equations (2) and (3).

## **2.2 Numerical Solution**

Numerical method was applied to solve Equations (2) and (3) due to it ability to replace all the terms of the differential equations with algebraic equations that can be easily solved. Particles of the grated unfermented cassava mash were represented by sphere of equivalent radius and moisture was assumed to move from the interior to the outward surface by diffusion. The computational domain represented the divisional region and was assumed that the system of the differential equation was valid over the finite difference domain as shown in Figure 1.

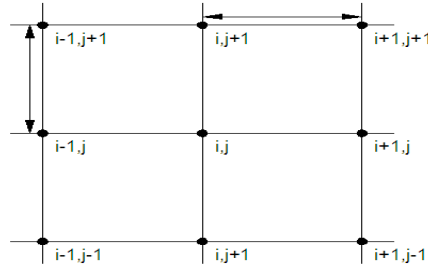


Figure 1: Grid Points for the Finite Difference Approximation.

where:  $i$ = radial grid index (1,2,3...n) ,  $j$ = time grid index(1,2,3...n)

Moreover, the proposed model assumes that the particle of the grated unfermented cassava mash consist of 'n' equal grids and sections of homogenous material with moisture profile noted at the interior section node lying between the centre and the outer surface of the particle respectively. The grid generation was accompanied by using directory ( $i$ ) in the direction  $R$ , therefore every nodes had it's axis and its expressed as (4) and (5).

$$R_i = i\Delta R - \frac{\Delta R}{2} \quad (4)$$

and

$$\Delta R = \frac{R_i}{n} \quad (5)$$

Therefore, Crank Nicholson Central Finite Difference Approximation method was chosen to solve equation (2) over the domain and is as stated in Equations (6), (7) and (8) (Jeffrey, 2011):

$$\frac{dM}{dt} = \frac{M_{i,j+1} - M_{i,j}}{\Delta t} \quad (6)$$

$$\frac{dM}{dr} = \frac{M_{i+1,j} - M_{i,j}}{\Delta R} \quad (7)$$

$$\frac{d^2M}{dr^2} = \frac{M_{i+1,j} - 2M_{i,j} + M_{i-1,j}}{\Delta R^2} \quad (8)$$

Substituting equations (6), (7) and (8) into equation (2) gave,

$$\frac{M_{i,j+1} - M_{i,j}}{\Delta t} = D \left[ \frac{M_{i+1,j} - M_{i,j}}{R_i \Delta t} + \frac{M_{i+1,j} - 2M_{i,j} + M_{i-1,j}}{\Delta R^2} \right] \quad (9)$$

Substituting  $R_i$  and  $\Delta R$  into Equation (9) and further solving using separation of variables resulted into the moisture content profile at different regions of the mash.

### 2.2.1 interior region the moisture content distribution:

$$\frac{M_{i,j+1} - M_{i,j}}{\Delta t} = \frac{n^2}{R^2} * \frac{4}{2i-1} [M_{i+1,j} - M_{i,j}] + D \frac{n^2}{R^2} [M_{i+1,j} - 2M_{i,j} - M_{i-1,j}] \quad (10)$$

Collecting like terms and making  $M_{i,j+1}$  the subject of the formula:

$$M_{i,j+1} = M_{i,j} + D \frac{n^2}{R^2} \Delta t \left[ \frac{4}{2i-1} M_{i+1,j} - \frac{4}{2i-1} M_{i,j} - 2M_{i,j} + M_{i+1,j} - M_{i-1,j} \right] \quad (11)$$

After solving the Equation (11),  $M_{i,j+1}$  which is the moisture profile at the interior nodes at a unit time intervals becomes:

$$M_{i,j+1} = M_{i,j} + D \frac{n^2}{R^2} \Delta t \left[ \frac{2i+3}{2i-1} M_{i+1,j} - \frac{4i+2}{2i-1} M_{i,j} + M_{i-1,j} \right] \quad (12)$$

### 2.2.2. The centre region moisture content distribution:

At the centre,  $r$  which is the radial position (m) = 0, i.e there is no moisture gradient at the center of the product the boundary condition is express as:

$$\left. \frac{dM}{dr} \right|_{r=0} = 0$$

Therefore, the term  $M_{i-1,j}$  in equation (12) equals to  $M_{i,j+1}$  in Equation (13) this is expressed as:

$$M_{i,j+1} = M_{i,j} + D \frac{n^2}{R^2} \Delta t \left[ \frac{2i+1}{2i-1} M_{i+1,j} + M_{i+1,j} - \frac{4i+2}{2i-1} M_{i,j} \right] \quad (13)$$

Further simplification of Equation (13) gave Equation (14) therefore, the moisture distribution at the center of the mash per unit time intervals gave:

$$M_{i,t+1} = M_{i,j} + D \frac{n^2}{R^2} \Delta t \frac{4i+2}{2i-1} (M_{i+1,t} - M_{i,j}) \quad (14)$$

### 2.3.4 The moisture distribution at the surface region

The following central finite difference approximation were employed to solve for the moisture distribution terms at the surface nodes where  $r = R$ :

$$\frac{dM}{dr} = \frac{2(M_{s,j} - M_{n,j})}{\Delta R} \quad (15)$$

And

$$\frac{d^2M}{dr^2} = \frac{2M_{n,j} - 3M_{n,j} + M_{n-1,j}}{\Delta R^2} \quad (16)$$

The algebraic form of equation (2) for the moisture distribution at the surface by substituting equations (15), (16),  $R$  and  $R_i$  with  $M_{n,j+1}$  becomes the subject of the formulae yielded:

$$M_{n,j+1} = M_{n,j} + D \Delta t \left[ \frac{n}{R} * \frac{4}{2i-1} * \frac{n}{R} (2M_{s,j} - 2M_{n,j}) + \frac{n^2}{R} (2M_{s,j} - 3M_{n,j} + M_{n,j}) \right] \quad (17)$$

where:  $s$  = at surface and  $n$  = number of hypothetical shell in the particles.

Further simplification by expansion of equation (17) gave (18):

$$M_{n,j+1} = M_{n,j} + D \frac{n^2}{R^2} \Delta t \left[ \left( \frac{4i+6}{2i-1} \right) M_{s,j} - \left( \frac{6i+5}{2i-1} \right) M_{n,j} + M_{n-1,j} \right] \quad (18)$$

To determine the moisture content at the surface ( $M_{s,j}$ ), Neumann boundary condition was considered for simplicity and accuracy. The convective boundary condition is express thus:

$$-D \frac{dm}{dr} = |sh_D (m_s - m_e) \quad (19)$$

where:  $H_D$ =mass transfer coefficient,  $M_s$ = Moisture content at the surface,  $M_e$ = equilibrium moisture content.

Substituting equation (18) into equation (19) yielded Equation (20):

$$-D \left[ \frac{2(M_{s,j} - M_{n,j})}{\Delta R} \right] = h_D (M_s - M_e) \quad (20)$$

Substituting for  $\Delta R$  in Equation (20) and expanding gave Equation (21).

$$M_{s,j} = \frac{Rh_D + 2M_{n,j}}{Rh_D + 2D_n} \quad (21)$$

Where:  $H_D$  = Mass transfer coefficient.  $R$  = radius of sphere (in the spherical coordinate)

Substituting for  $M_{s,j}$  in equation (21) gave the moisture distribution at the surface region as Equation (22)

$$M_{n,j+1} = M_{n,j} + D \frac{n^2}{R^2} \Delta t \left[ \left( \frac{4i+6}{2i-1} \right) \left[ \frac{Rh_D M_e + 2M_{n,j}}{Rh_D + 2D_n} \right] - \left( \frac{6i+5}{2i-1} \right) M_{n,j} + M_{n-1,j} \right] \quad (22)$$

### 2.2.3 Determination of Mass transfer coefficient $h_D$

$H_D$  is the mass transfer coefficient which describe the convective mass transfer that occurred at the surface of the material and was calculated via Sherwood number (Patil, 2008) as revealed by Equations (23) to (27);

$$Sh = \frac{h_D d}{D_w} \quad (23)$$

$$h_D = \frac{sh D_w}{d} \quad (24)$$

where:  $d$  = diameter of mash,

$D_w$  = diffusion coefficient of water vapour in air =  $2.20 \times 10^{-5} \text{ m}^2/\text{s}$ .

$$Sh = 2.0 \text{ } \dot{G} 0.552 R_e^{0.53} \text{ } \dot{G} S_c^{0.33}, \quad (25)$$

$$R_e = \frac{u d \rho}{\mu} \quad (26)$$

$$S_c = \frac{\mu}{\rho d} \quad (27)$$

Where:  $u$  = mass velocity of air ( $\text{kg} \cdot \text{m}^{-2} \cdot \text{s}$ ),  $d$  = particle diameter (m),  $\rho$  = density  $\text{kg}/\text{m}^3$ ,  $\mu$  = viscosity of air. ( $\text{kg s}^{-1} \text{ m}^{-1}$ ).

### 2.2.4 Determination of Equilibrium moisture content

Modified Henderson Equation was applied due to simplicity and extensive application in the moisture sorption isotherm models as given by Equation (28) (Wihelm *et al.*, 2005).

$$rh = 1 - \exp[-A(T + C)M_e^B] \quad (28)$$

**2.2.5 Determination of the average moisture content**

Trapezoidal Rule of integration was adopted in solving equation (3) and this yielded the average moisture content. (Patil, 2008, and Jeffry, 2011). Trapezoidal rule is defining as a rule for estimating area of irregular figure by dividing it into parallel strips of equal width, each strips forms a trapezium. It can also be adapted to obtain an approximate value of a definite integral. (Collins 2014). Figure 2.1 showed the graphical representation of the trapezoidal rule is as shown

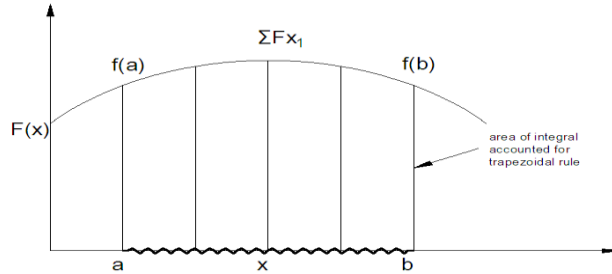


Figure 2: Graphical Representation of the Trapezoidal Rule (Jeffry, 2011)

The cross section sphere representing the particle of the grated mesh is assumed to like a graphical representation of the trapezium. From Figure 1, the area under the curve was determined by adding the area of the trapezoids and the base is assumed to be the height.

i.e.  $h = \Delta x$ . Total area is express thus in Equation (29):

$$\int_b^a f(x)dx = \frac{h}{2} [f(a) + f(b) + 2 \sum_{i=2}^n f(x_i)] \tag{29}$$

**2.2.6 The average moisture content at the interior of the region**

$f(a)$  is the summation of the average moisture content at the interior region and the position of the left side of the  $i^{th}$  trapezoid became  $x_i$ . Therefore,  $a_i =$  area of each trapezoids and express as shown in Equation (30):

$$= \frac{h}{2} [f(x_i) + f(x_i + h)] \tag{30}$$

Considering the coordinates of grated mesh, area is express as Equation (31):

$$f(x) = \frac{\Delta R}{4} [R_{i,j}^2 M_{i,j}] \tag{31}$$

where:  $R = 0$  and  $i=1$ ,  $R_i = \frac{R}{n} * \frac{2i-1}{2}$ ,  $\Delta R = \frac{R}{n}$

Substituting for R yielded the average moisture content at the center of the particles which is indicated as Equation (32):

$$f(x) = \frac{R^3}{16n^3} (2i - 1)^2 \tag{32}$$

**2.2.7 The average moisture content at the center region:**

$2 \sum_2^n f(x_i)$  is the summation of the average moisture content at the center region where  $i < 1 < n$ .

$$f(x) = \frac{\Delta R}{2} [R_{i,j}^2 M_{i,j} + \sum_{i=2}^{n-1} \Delta R (R_{i,j}^2) + \frac{\Delta R}{2} (R_{n,j}^2 M_{n,j})] \tag{33}$$

Substitute for  $R_i$  and R, after expansion, yielded average moisture content at the interior node in Equation (37):

$$f(x) = \frac{8}{R_n^3} (2i - 1)^2 M_{i,j} + \frac{R^4}{4n^4} \sum_{i=2}^{n-1} (2i - 1)^2 M_{i,j} + \frac{R^4}{16n^4} (2i - 1) M_{n,j} \quad (34)$$

### 2.2.8 The average moisture content at the surface. is expressed thus

$f(b)$  is the summation of the average moisture content at the surface region and this is the position of the right side of the  $i^{\text{th}}$  trapezoid gave Equation (35):

$$f(x) = \frac{\Delta R}{4} [R_{n,j}^2 M_{n,j} + R_{max}^2 M_{s,j}] \quad (35)$$

Substituting for  $\Delta R$  in Equation (35) gave the average moisture content at the surface region as seen in Equation (36):

$$f(x) = \frac{R}{16n^3} (2i - 1)^2 M_{n,j} + \frac{R^3}{4n^3} M_{s,j} \quad (36)$$

$M_{s,j}$  represent the moisture at the surface which can be evaluated without considering the convective mass transfer which occur at the surface of the material and is determined via Sherwood number Sh (Bryan and Brian 1996). Therefore, summation of Equations (32), (34) and (36);

$$\bar{M} = \frac{3}{R^3} \left[ \frac{3R^3}{16n^3} [M_{i,j} + (2n - 1)^2 M_{n,j}] + R^3 \left[ \frac{M_{n,j}}{4n+sh} + \sum_{i=2}^{n-1} (2i - 1)^2 M_{i,j} \right] \right] \quad (37)$$

$\bar{M}$  = Average moisture content (% , db)

A computer programme written in Visual Basic programming was used to solve the set of equations (15, 17, 25 and 40) and to simulate moisture diffusion within the particles of the grated unfermented cassava mash and to compute average moisture content of the particle at unit time intervals. The input parameters of the simulated program are the number of concentric shell of equal thickness of which product particle was divided, the initial moisture content, the air, water and cassava mash properties. An empirical equation to calculate moisture diffusivity as a function of material temperature and moisture content, equations for computing Sherwood number, mass transfer coefficient and equilibrium moisture content. Flowchart of algorithm for the drying process of the industrial cassava mash is as shown in Figure 2.



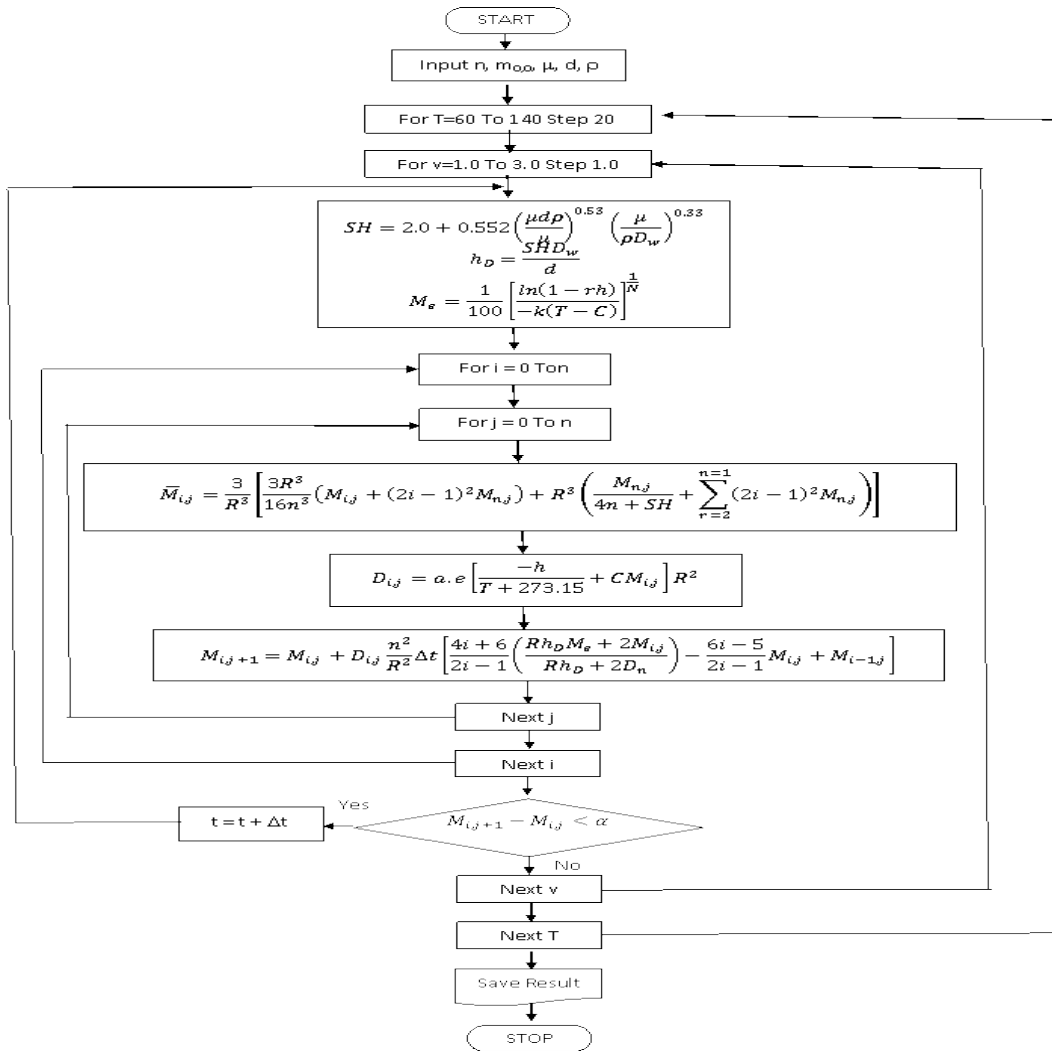


Figure 3: Flowchart of Algorithm for the Drying Process of Industrial Cassava Mash

### 2.3 Computer Programme Structure and Features

The algorithm in Figure 2 aided in the writing of a computer programmed named “crop-drying simulator 1.0”. The was made up of software interface where by the user input all the necessary parameters required for the simulation of the average moisture distribution in the product during drying through series of iteration steps until convergence took place. Convergence was assumed whenever the difference between the values of two successive iteration steps were less than ten. Crop drying simulator interfaces divided into three section: the parameter section, the command section and the result section.

The command section consists of the execute command button, export command button and the close command button. The execute command button is clicked when all necessary parameters are properly entered in the parameter section. Clicking on the execute command button, the result of the simulation is displayed in the result section. The result section is in tabular form. It consists of columns for the display of time, observed values, simulated values and difference. The close command button shut down the programme. Figure 3 is the computer drying simulator 1.0 interface with the display of results.

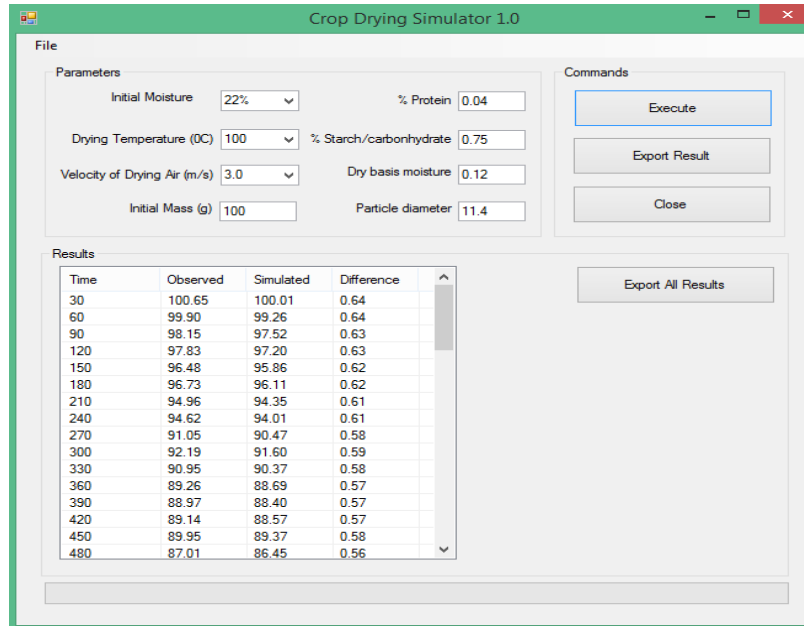


Figure 4: Computer Programme Crop-drying Simulator 1.0 Interface with display.

### 3. Materials and Methods

The materials used for the experimental investigation included: (i). the grated unfermented cassava mash (ii). Model laboratory dryer with full instrumentation. The experiment was carried out at the Engineering and Materials Testing laboratory of the Engineering and Scientific Services (ESS) department of the National Centre for Agricultural Mechanization (NCAM), Ilorin, Kwara State Nigeria.

#### 3.1 The grated unfermented cassava mash.

The cassava tubers were obtained from the NCAM farm and was processed into cassava mash as shown in the flow diagram in Figure 5.

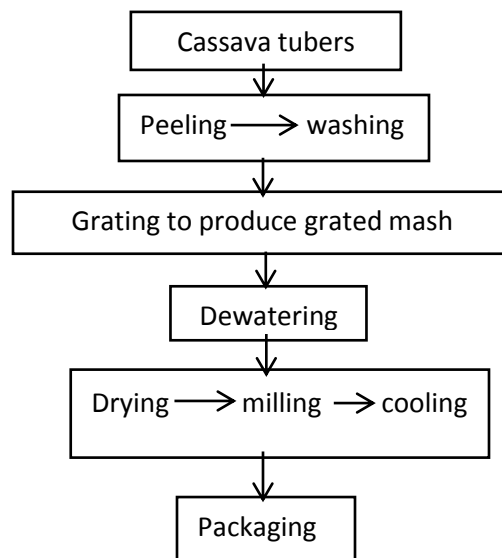


Figure 5: Flow temperature controller K - type, model WRX – 31 chart Showing the Production Process of Industrial Cassava Flour

### 3.2 Description of the Model Laboratory Dryer

A laboratory Model Dryer with full instrumentation was used for the drying process of the grated unfermented cassava mash after dewatering process as displayed on the flow diagram. The dryer consisted of an aluminium Load Cell (OIML), a voltage/frequency AC motor speed controller, a temperature controller K-type model WRX – 31, and a TC-08 Thermocouple Data Logger. A sample tray was hanged to the load cell for monitoring of the rate of moisture remover during drying at an interval of 30 seconds and readings were displayed on the interface of a personal computer. The motor speed controller was used for the variation of air flow rate and the K-type temperature controller was used for the variation of dryer temperature. The K-type thermocouples monitored the temperature of the sample at 8 different points in the sample tray and the readings were logged into the personal computer via the TC-08 data logger. The power rating of the dryer's fan motor is 0.75kW. The heat source is from 2kW electric heater powered by 230 Volt AC supply via the temperature controller. The model dryer with the associate instrumentation is as shown in Figure 6.



Figure 6: Dryer with Associated Instrumentation

### 3.3 Drying Procedure

The Experimental Model dryer was pre-set to desired temperature with the use of the temperature controller and left until the inside temperature of the dryer reached the pre-set value which is displayed on the personal computer. This indicated the readiness of the dryer for the drying procedure.

Samples were weighted on a sensitive scale in order to record the initial weight of the sample after which it was carefully placed on the sample tray in the dryer which was hanged to the load cell to monitor the amount of moisture being removed from the sample. The door of the dryer was locked and the rate of removal of the moisture was displayed at interval of 30 seconds on the screen of the personal computer. The process continued until the readings displayed on the interface became constant.

### 3.4 Validation of the Finite Difference Developed Model

The summary simulated values of moisture content and the experimental values are as shown above. Graphical presentation and statistical analysis were used for the validation procedure. The Model predictions were evaluated on the bases of Root Mean Square Difference (RMSD) (Niroot, 2010).

$$RMSD = \frac{\sqrt{\frac{\sum_{i=1}^N (y_{sim_i} - y_{meas_i})^2}{N}}}{\frac{\sum_{i=1}^N y_{meas_i}}{N}} \times 100 \quad (38)$$

Where  $y_{sim}$  and  $y_{maes}$  are the predicted and measured values of variables  $y$  respectively.  $N$  is total number of data.

### 3.5 Moisture Diffusivity

Moisture diffusivity was determined according to Bhagwati and Prakash (2011). RMSE was computed using Equation 39.

$$RMSE = \sqrt{\frac{\sum_{i=1}^n (M_{ei} - M_{pi})^2}{n}} \times 100 \quad (39)$$

Where,  $M_{ei}$  and  $M_{pi}$  are experimental average moisture (% d.b) and model predicted average moisture (%d.b) at a given time period respectively.  $n$  represent the number of time period used to calculate RMSE.

### 3.0 Result and Discussion

Table 1: Summary of Statistical Analysis of the Experimental and Simulated Results of Moisture Content

	N	Range	Minimum Mean value of M/C(%db)	Maximum mean value of M/C (%db)	Sum	Mean	Standard Deviation	Variance
RMSD	125	0.506	0.337	0.844	73.397	0.587	0.096	0.009
DIFF	125	0.406	0.260	0.667	57.631	0.461	0.073	0.005

RMSD : Root Mean Square Method

DIFF : Difference in the moisture content of the simulated and experimental results

From Table 1, the mean value of the Root Mean Square Difference RMSD is 0.59%. This is within the acceptable limit which is 10%. (O'Callaghan, 1971 and Nirroot, 2010). Thus the prediction is very good.

### 4.2 Comparison of the Simulated and the Experimental Drying Kinetics

Figure 6a- 6e showed the comparison between the simulated and the experimental values of the moisture distribution within the unfermented grated cassava mash particles at typical air temperatures of 40°C, 55°C, 70°C, 85°C and 100°C.

From Figure 6a-6e it can be observed that the moisture content of the unfermented grated cassava mash decreases as the drying time increases until equilibrium moisture content was attained. The graphical representation of the comparison showed that both the simulated and the experimental exhibit the same trend. Hence, the simulated and the experimental result showed reasonably close agreement. This is in agreement with other works carried out by other researcher on the drying of agricultural materials (Balaban and Pigott, 1988; Afolabi, 2014).

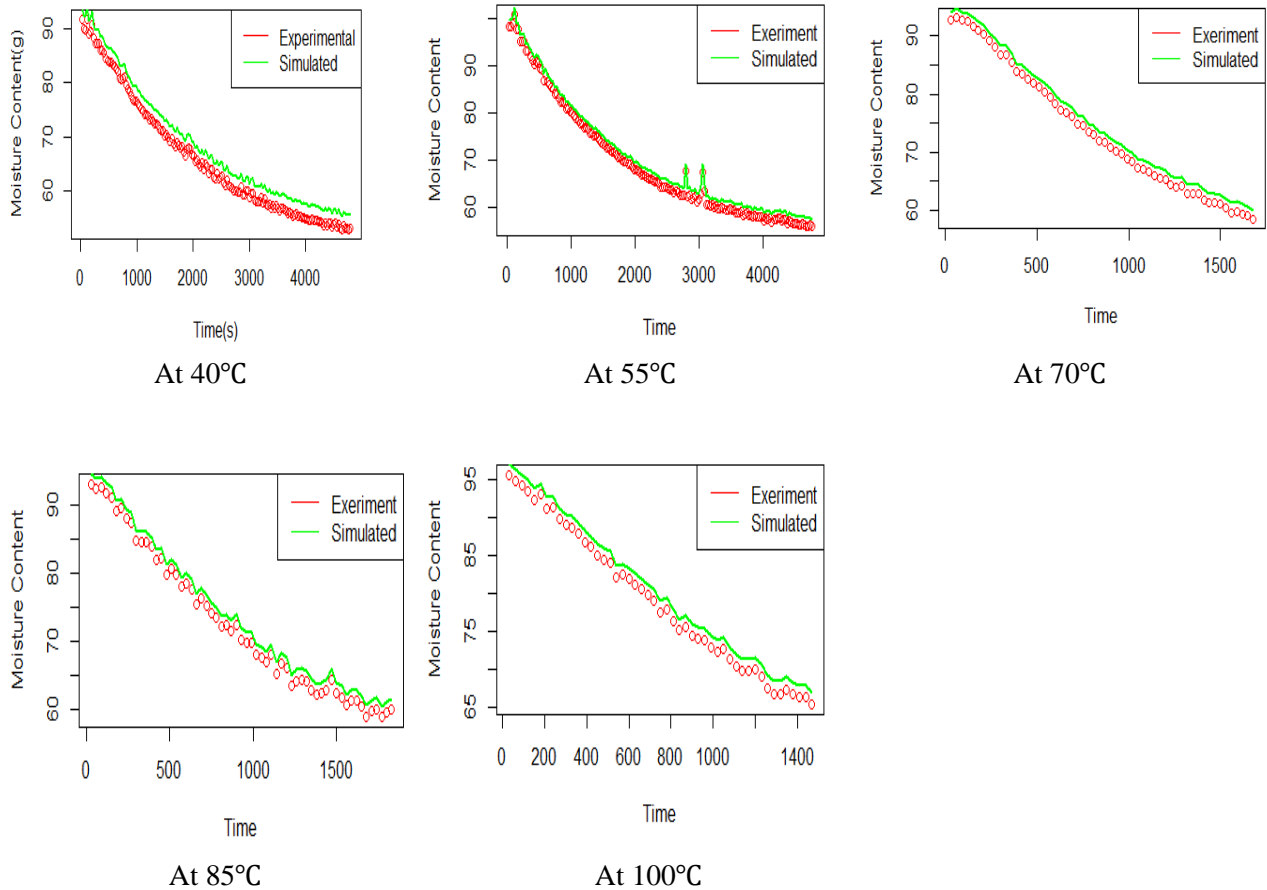


Figure 6a-6e: Experimental and simulated variation of moisture content with time at different temperature level

### 4.3 Drying Time

From the experiment, the average time of drying was evaluated and the Table 2 shows the summary of the statistical analysis of average time of drying at different temperature level

Temp of drying (°C)	Meandryin g time Std. Error		95% Confidence Interval	
			Lower Bound	Upper Bound
40	2.565	.166	2.235	2.895
55	1.817	.166	1.487	2.147
70	1.471	.166	1.141	1.801
85	1.307	.166	.977	1.637
100	1.252	.166	.922	1.583

From the Table, it was observed that the time of drying reduced with increase in temperature levels. At the lowest temperature level 40°C, the highest average time of drying was observed to be 2 h, 57min. similar trend was noticed with temperature level 55°C which had average time of drying as 1h, 82 min. Also similar trend observed with by temperature levels 70°C, and the average time of drying was 1h, 47 min. At the next temperature level which is 85°C, the time of drying was 1 hour: 30 minutes. The highest

temperature level, which is 100°C, the average time of drying, was 1 h, 25 min. This trend was reasonable because, in this study, it was assumed that the mechanism of the drying process is predominantly controlled by liquid diffusion. In this study, it was assumed that the mechanism of the drying process is predominantly controlled by liquid diffusion under concentration gradient and this gradient can be caused by evaporation or as a result of capillary forces (Dilip and Parikh, 2014). In mass transfer, one or more components are often being transported by relative motion through one another (Mujumdar, 2008).

The cause of this molecular motion is the concentration gradient where the net flux of diffusion process is from a region of high concentration to a region of low concentration (Mujumdar, 2008). In the diffusion of gases or the diffusion of a solute in a dilute solution, the molecules of the diffusing substance rarely collide with each other due to the tremendous spacing among the diffusing molecules (Dimitrios, *et al.*, 2014). According to the kinetic theory, temperature is the expression of the average energy of molecular motion. Water molecules with high kinetic energy will escape from the liquid water surface against the cohesive force that binds the molecules in liquid water (Carvalho *et al.* 2014). The process by which matter is transported from one part of a system to another part is a result of random molecular motion, also known as random walk. (Jaruk and John, 2007). As soon as this occurred, the remaining molecules redistribute their energy by collision for continuous random walk (Kaisa *et al.*, 2004).

Therefore the higher the temperature of drying air, the larger the kinetics energy of the water molecules which enable the escape from the liquid water surface of grated mash thus, reduction in the time of drying. Moreover, in the interior of the liquid, a molecule is completely surrounded by other liquid molecules which are attracted to it in every direction. As temperature increases the concentration of the vapour phase increases, and the surface tension decreases and this enable the release of the liquid molecule to the environment in form of vapour (Saneinejad *et al.*, 2012). Therefore, higher air temperature removed moisture at a faster rate because internal moisture migration increases as the heat flux increases and drying time decreases (Doymaz and İsmail, 2011, Motevali *et al.*, 2014).

## **5. Conclusion**

The following conclusions can be deduced from this study that:

- i. The developed mathematical model is a useful tool for predicting the drying kinetics of industrial cassava flour and can also be used for numerical parameter estimation of some properties of industrial cassava flour that are difficult to measure experimentally.
- ii. The higher the temperature, the higher the drying rate and the lower the time of drying. Hence, the drying process of unfermented grated cassava mash occurred in the falling rate-drying period.
- iii. The mean value of the Root Mean Square Difference (RMSD) between the simulated and the experimental was within the acceptable limit. Showing that there was close agreement between the simulated and the experimental moisture content data.

## **REFERENCES**

Adebayo, K., Lamboll, I. and Westby, A. 2009. Contextualizing Environmental, Social and Behavioral Issues in the Cassava Post-harvest System in Africa. *Anthropologist Special Volume No. 5: 137-146.*

Adejumo, AL, Aderibigbe, AF and Layokun, SK `2011. Cassava Starch: Production, Physicochemical Properties and Hydrolysatation journal of advances in Food and Energy Security 2 8-17.

Ajala, AS., Aboiye, AO, Popoola, JO. and Adeyanju, JA. 2012. Drying Characteristics and Mathematical Modelling of Cassava Chips. Chemical and Process Engineering Research [www.iiste.org](http://www.iiste.org) ISSN 2224-7467 (Paper) ISSN 2225-0913 (Online) Vol 4,

AOAC., 1990. Official Methods of Analysis. Association of Official Analytical chemists, Washington DC. USA.

Bhagwati P., 2011 .Mathematical Modeling of Moisture Movement within a Rice Kernel during Convective and Infrared Drying. A Ph.d dissertation submitted to Biological Systems Engineering. University of California.

Carvalho, WT., Oliveira, TF., Silva, FA., Caliari, M., and Soares Júnior, M. (2014). Drying kinetics of potato pulp waste. Food Science and Technology, 34(1), 116-122. <http://dx.doi.org/10.1590/S0101-20612014000100017>.

Cassava: Adding Value for Africa (C: AVA) 2010: University of Greenwich, natural resources institute.

Crank, J and Nicolson, P. 1947. A practical method for numerical evaluation of solutions of partial differential Equations of the heat conduction type". Proc. Camb. Phil. Soc. 43 (1): 50–67

Datta, A. 2008. Status of Physics-Based Models in the Design of Food Products, Processes, and Equipment, Comprehensive Reviews in Food Science and Food Safety, Vol. 7 No. 1

Dimitrios, AT, Zempelikos AN, Alexandros PVB., Achilleas VBB., Andronikos EF C, 2011 ; Journal of Medicinal Plants Research Vol. 5(19), pp. 4721-4730, 23

Doymaz, I. 2010. Evaluation of Mathematical Models for Prediction of Thin-Layer Drying of Banana Slices. International Journal of Food Properties, 13, 486-497.

Doymaz , I and İsmail, 2011 Drying characteristics of sweet cherry Food Bioprod. Process, 89 pp. 31–38.

Gaston, AL., RM. Abalon and SA. Giner, 2002. Wheat Drying Kinetics. Diffusivities for Sphere and Ellipsoid by Finite Element. Journal of Food Engineering, 52: 313-322

Gatea, AA. 2011. Design and construction of a solar drying system, a cylindrical section and analysis of the performance of the thermal drying system. African Journal of Agricultural Research, 6, 343–351.

Jaruk, S. and John SR, 2007; Moisture Transfer in Solid Food Materials: A Review of Mechanisms, Models, and Measurements International Journal of Food Properties, 10: 739–777, 2007 Copyright © Taylor and Francis Group, LLC ISSN: 10942912 print / 1532-2386 online DOI: 10.1080/10942910601161672739 Department of Food Science and Technology, Cornell University, Geneva, NY, USA Western Regional Research Center, Agricultural Research Service, United States Department of Agriculture, Albany, CA, USA

Jia, C., Sun, DW. and Cao, CW. 2000. Mathematical Simulation of Temperature and Moisture Fields within a Grain Kernel during Drying. Drying Technology, 18 (6): 1305-1325. 22.

*Adejumo and Oje: Simulating the Drying Kinetics of Cassava Flour in a Laboratory Model Dryer Using Finite Difference Method. AZOJETE, 13(5):577-592. ISSN 1596-2490; e-ISSN 2545-5818, [www.azojete.com.ng](http://www.azojete.com.ng)*

Luikov, AV. 1966; Heat and Mass Transfer in Capillary-Porous Bodies; Pergamon Press: Oxford.

Kadi, H. and Hamlat, MS., 2002. Studies on drying kinetics of olive foot cake. *Grasesy Aceites*, 53, 226–228.

Moorthy, SN., 2002. Tuber crop starches, Tech. Bull. No 18, CTCRI, Trivandrum, p. 52.

Mujumdar, AS., 2008. Guide to Industrial Drying, Ed. Mujumdar, A.S., Three S Colors.Publication, Mumbai, India.

Mujumdar, AS., 2006. Hand book of industrial drying. CRC Press, Boca Raton, USA.Othman, M.Y.H.;

O'Callaghan, JRO, Menzies, D.J, Bailey 1997.P.H simulation of agricultural engineering Research 1971, 16, 223-244. Pal U.S and chakraverty. A thin-layer convection drying of mushroom. *Energy conservation and management*. 38(2)107-113.

Patil, ND. 2006. Evaluation of diffusion Equation for simulating moisture movement within an individual grain kernel. *Drying Tech*. 6(1): 21-42.

Rafiee, S., Jafari, A., Kashaninejad M. and Omid, M. 2007. Experimental and Numerical Investigations of Moisture Diffusion in Pistachio Nuts during Drying with High Temperature and Low Relative Humidity. *International Journal of Agriculture and Biology*, 9 (3): 412-415

Wihelm, Luther, R, Dwayne A.,Suter and Geraid H Brusewitz 2005. Drying and dehydration. Chapter 10.Food and process Engineering technology, 259-284.StJoseph, Michigan. ASAE.